Organic & Biomolecular Chemistry

www.rsc.org/obc

Volume 6 | Number 21 | 7 November 2008 | Pages 3865–4068

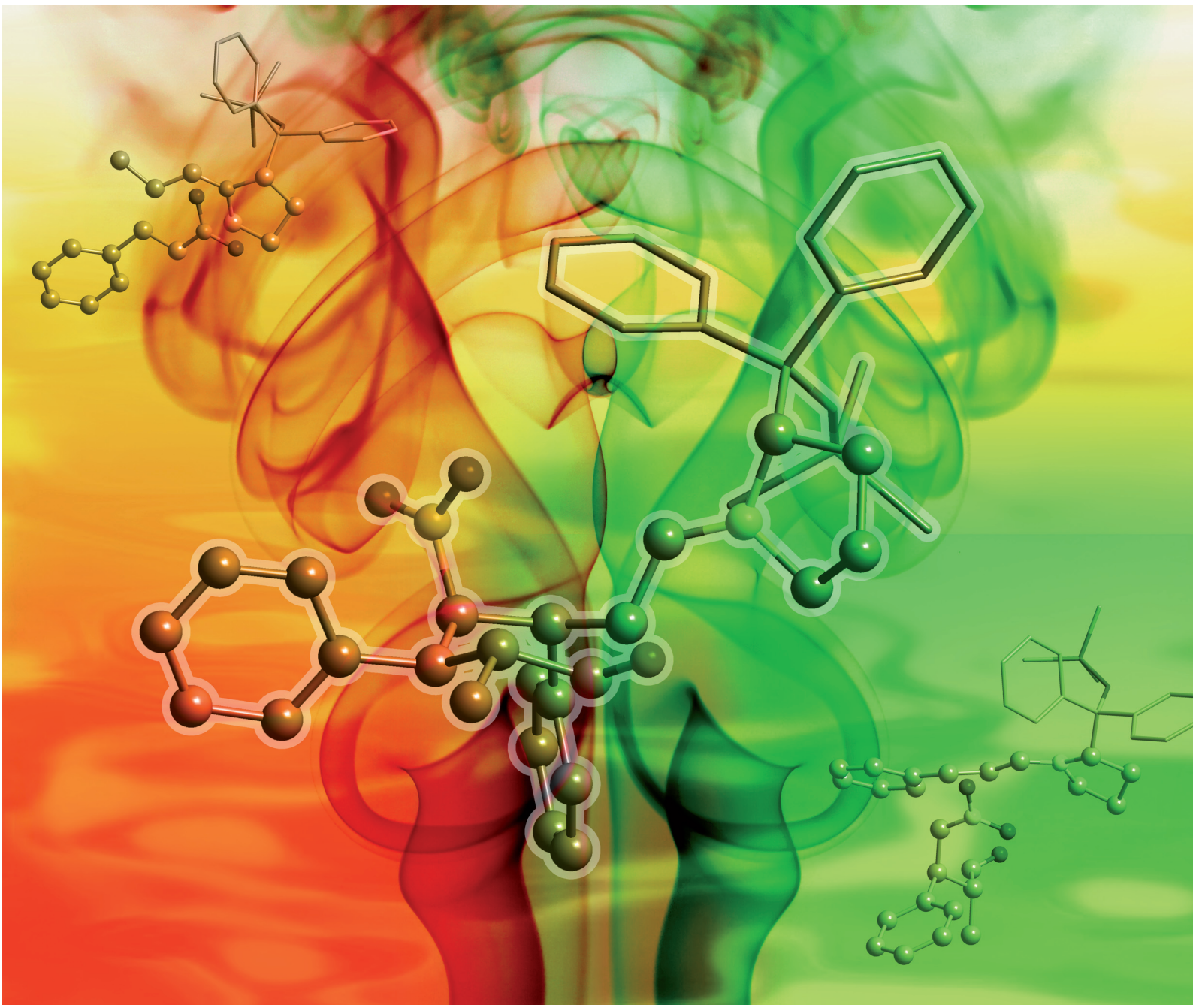

ISSN 1477-0520

RSC Publishing

FULL PAPER

C. B. Shinisha and Raghavan B. Sunoj
Unraveling high precision stereocontrol in a triple cascade organocatalytic reaction

Chemical Biology

In this issue...

1477-0520(2008)6:21;1-J

Unraveling high precision stereocontrol in a triple cascade organocatalytic reaction†

C. B. Shinisha and Raghavan B. Sunoj*

Received 26th June 2008, Accepted 13th August 2008
First published as an Advance Article on the web 12th September 2008
DOI: 10.1039/b810901j

The mechanism and stereoselectivity in an organocatalyzed triple cascade reaction between an aldehyde, electron deficient olefin and an α,β-unsaturated aldehyde are investigated for the first time using density functional theory. The factors responsible for high levels of observed stereoselectivity (Enders *et al., Nature,* 2006, **441**, 861) towards the generation of cyclohexene carbaldehyde with four contiguous stereocentres are unravelled. The triple cascade reaction, comprising a Michael, Michael and aldol sequence as the key elementary reactions, is studied by identifying the corresponding transition states for the stereoselective C–C bond-formation. In the first Michael addition step between the enamine (derived from the chiral catalyst and propanal) and nitrostyrene, energetically the most preferred mode of addition is found to be between the *si*-face of (*E*)-*anti*-enamine on the *si*-face of nitrostyrene. The addition of the *si*-face of the nitroalkane anion on the *re*-face of the iminium ion (formed between the enal and the catalyst) is the lowest energy pathway for the second Michael addition step. The high level of asymmetric induction is rationalized with the help of relative activation barriers associated with the competitive diastereomeric pathways. Interesting weak interactions, along with the steric effects offered by the bulky α-substituent on the pyrrolidine ring, are identified as critical to the stereoselectivity in this triple cascade reaction. The predicted stereoselectivities using computed energetics are found to be in perfect harmony with the experimental stereoselectivities.

Introduction

Asymmetric multicomponent domino reactions have emerged as a powerful strategy for the synthesis of complex molecules with multiple stereocentres. The synthetic potential of domino reactions has been utilized in efficient and stereoselective construction of several targets, starting from relatively simple precursors.[1] Most significantly, the creation of many stereocentres is possible by using a single catalyst in *one pot*, without the isolation of intermediates or changing the reaction conditions. These domino reactions are reminiscent of biomimetic pathways, as they resemble the biosynthesis of complex natural products from simple precursors as building blocks.[2]

The recent overwhelming activities in organocatalysis[3] have set the stage for a number of interesting organocatalytic cascade reactions towards the construction of complex molecular structures.[4] The organocatalytic cascade reactions are often accompanied by high levels of stereocontrol achieved through chiral organocatalysts. The successful implementation of organocatalysts in cascade reactions can generate functionalized polycyclic bioactive molecules.[5] Among current organocatalysts, chiral secondary amines are more frequently employed to activate substrate(s) as enamine/iminium species, which in turn can participate in a range of reactions with a multitude of electrophiles.[6] The intermediates thus generated may not be stable enough and amenable for isolation, but permit quick transformation into more stable products through a subsequent reaction sequence. The stereoselectivity of these reactions is controlled in the bond formation step, either through hydrogen bond directed Brønsted acid catalysis as in proline[7] or a steric control approach as in diphenyl prolinol ethers.[8] The combination of different activation modes allows the design of innovative domino sequences to tackle high level stereochemical complexity of desired targets. Therefore, the organocatalytic reactions can ideally be exploited in designing tandem processes.

In a very recent study, Enders and co-workers have demonstrated an elegant asymmetric organocatalytic triple cascade reaction involving a linear aldehyde (**A**), a nitroalkene (**B**) and an α,β-unsaturated aldehyde (**C**) towards constructing a tetrasubstituted cyclohexene carbaldehyde with a high degree of diastereoselectivity and complete enantiocontrol.[9] The reaction, as shown in Scheme 1, employed diphenylprolinol trimethylsilyl ether as the catalyst. It is also of interest to note that recently, diphenyl siloxy proline ethers have successfully been used as catalysts in a variety of reactions,[10] including cascade reactions.[11] Enders's triple cascade reaction is an exquisite example that includes the advantages of domino reactions as well as asymmetric organocatalysis. It should be noted that a suitably designed cascade reaction of this kind could open up convenient inroads into several polyfunctional cyclohexene building blocks with high levels of stereocontrol.

The present cascade reaction involves two conjugate additions followed by an intramolecular aldol cyclization. The first step is a Michael addition between propanal and nitrostyrene. The catalyst forms a chiral enamine with the aldehyde (**A**), which subsequently

Department of Chemistry, Indian Institute of Technology Bombay, Powai, Mumbai, 400076, India. E-mail: sunoj@chem.iitb.ac.in; Fax: 91-22-2572-3480 or 91-22-2576-7152

† Electronic supplementary information (ESI) available: The optimized geometries of all the transition states in the form of Cartesian coordinates, Figures S1–S4 and Tables S1–S10. See DOI: 10.1039/b810901j

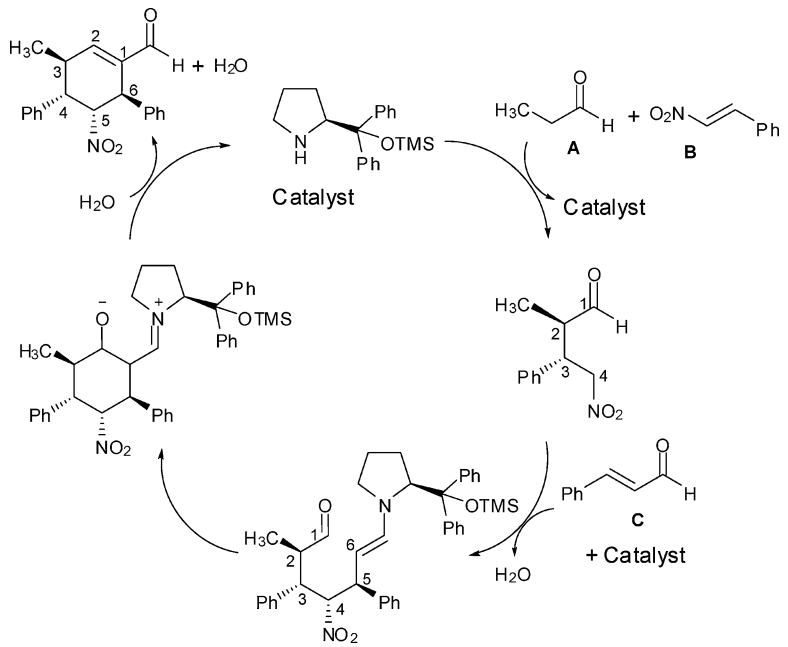

Scheme 1 Proposed catalytic cycle for the diphenylprolinol trimethylsilyl ether catalyzed triple cascade reaction for the generation of tetrasubstituted cyclohexene carbaldehydes.

adds to the nitroolefin.[12] A number of chiral pyrrolidines without a proton donating group have been remarkably successful in giving good yield and high enantioselectivity in such conjugate additions.[13] Here, the higher reactivity of the nitroolefin with the activated aldehyde can help supercede the possible iminium ion formation between the catalyst and the available α,β-unsaturated aldehyde. After the first Michael addition, the catalyst liberated on hydrolysis can form an iminium ion[14] with the α,β-unsaturated aldehyde (**C**) to accomplish the conjugate addition with the nitroalkane formed in the first step.[15] In the third step, the enamine intermediate formed from the second step undergoes cyclization through an intramolecular aldol reaction. The subsequent aldol cyclization and hydrolysis release the tetrasubstituted cyclohexene carbaldehyde. Enders *et al.* have further extended this domino reaction for the synthesis of poly substituted bicyclic and tricyclic carbon frameworks.[16]

Albeit qualitative proposals on the plausible mechanism of this organocatalytic cascade reaction are documented, clear insights into how such precise stereocontrol arises are evidently not reported. In this triple cascade reaction, four contiguous stereocentres are generated with such high precision that only two epimers are isolated out of 16 possible stereoisomers. Such remarkable stereocontrol prompted us to probe the origins of observed high stereoselectivity. As part of our ongoing efforts to understand stereoselectivities in organocatalytic reactions,[17] we have decided to investigate the energetics as well as the controlling factors contributing to stereoselectivity using computational methods. The present study offers the first comprehensive report on the stereoselectivity in organocatalytic cascade reactions. The insights obtained through modeling of experimentally known examples could later be utilized for rational design of new organocatalysts suitable for domino reactions. Also, the insights could help design cascade reactions towards specific target molecules with considerable structural and stereochemical complexity.

Computational methods

A full DFT calculation on the present reaction, consisting of a fairly large number of atoms, will evidently be costly. On the other hand, semi-empirical approaches could be flawed by an imperfect description of the transition states leading to poorer energetic estimates. We have therefore used a combination of density functional theory (B3LYP/6-31G*) and semi-empirical MO methods (AM1) with a hybrid ONIOM2 scheme denoted as ONIOM2(B3LYP/6-31G(d):AM1) using the Gaussian03 suite of quantum chemical programs.[18,19] In the ONIOM2(B3LYP/6-31G(d):AM1) approach, the energy of the *real* system at the *high* level can be estimated using an extrapolation scheme as, E (ONIOM,*real*) = E (*high*,*model*) + E (*low*,*real*) − E (*low*,*model*). This approach has been successful in explaining the mechanism as well as stereoselectivity of organic reactions.[20]

The geometry optimizations of reactants, intermediates, transition states and products were carried out using the ONIOM2 method described above. All of the transition states were characterized as first order saddle points and the imaginary frequencies were confirmed to represent the desired reaction coordinate. Additionally, we have carried out 10% displacement of the transition state geometry along the direction of the imaginary vibrational frequency and subsequently reoptimized the perturbed structure using the "calcfc" option available in the program. This was to ensure whether the transition state is genuine and connects reactants and product. The single-point energies were subsequently calculated at the B3LYP/6-31G* level[21,22] using the ONIOM2 optimized geometries. The DFT single-point energies are used throughout the manuscript, unless otherwise specified.

According to the general recommendations given by Morokuma *et al.* for a multi-layer hybrid calculation, a substituent value test (*S-value test*) is performed. This is to examine how good the partition scheme and the corresponding model chemistries are for

the present system. The *S*-value is defined as *S* (level) = *E* (level, real) – *E* (level, model). The *S*-value is determined on the basis of the relative energies of **TS-1f** and **TS-1a** (*vide infra*). The Δ*S* (high) and Δ*S* (low) are respectively found to be only 0.07 and 1.04 kcal mol^{-1}. The error associated with the ONIOM extrapolation is therefore ($E_{(ONIOM,real)}$ – $E_{(high, real)}$) estimated as 0.97 kcal mol^{-1}, which is well within the recommended error tolerance limit of 2 kcal mol^{-1}.[18b]

Results and discussion

The stereoselectivity of the triple cascade reaction is studied by focusing on the critical C–C bond-formation steps. First, a fully optimized geometry of the catalyst obtained at the B3LYP/6-31G* level is partitioned into two layers for subsequent optimization using the ONIOM2 method. The most crucial part of the reacting system (inner layer) is described using the density functional theory while the pyrrolidine α-substituent (diphenyl (trimethyl)siloxymethyl group) is treated as the outer layer using the semi-empirical AM1 method.[23] The resulting dangling bond between the model system and the remainder of the molecule is saturated using a link atom. The geometric parameters of the catalyst optimized separately using the B3LYP/6-31G* and ONIOM2 are found to be in good agreement with each other.[24] The lowest energy conformer of the catalyst with the same layering scheme is chosen for further calculations of the cascade reaction sequence using the ONIOM2 approach.[25]

For the Michael addition step between propanal-enamine and nitrostyrene,[26] multiple modes of approach are possible. We have considered additions involving the sterically unhindered face of the enamine intermediate on both the *re* and the *si* faces of (*E*)-nitrostyrene.[27] The enamine derived from propanal and the catalyst can have four key conformers arising from the *E*/*Z* configuration of the enamine double bond as well as the *syn*/*anti* orientations. The *syn* and *anti* descriptors denote the orientation of the enamine double bond with respect to the α-substituent on the pyrrolidine ring. These notations would be used hereafter to specify the enamine double bond orientations. In the addition step, the transition states are expected to maintain a staggered orientation of the substituents around the incipient C–C bond. The *re*/*si* face of (*E*)-nitrostyrene and enamine may adopt six staggered orientations around the developing C–C bond. Considering the four key conformers of enamine, the first step of the cascade cycle can have 24 transition states. The geometry optimization of various enamine configurations and conformers reveals that the *Z* isomer is in general higher in energy than the corresponding *E* isomer in both *syn* and *anti* enamines. In particular, the (*Z*)-*syn*-enamine is found to be 10.7 kcal mol^{-1} higher in energy than the (*E*)-*anti*-enamine at the B3LYP/6-31G* level of theory.[28] Further investigations therefore exclude (*Z*)-*syn*-enamine, leaving behind 18 key transition states leading to four possible diastereomeric products. A representative set of these transition state possibilities for the addition of (*E*)-*anti*-enamine to (*E*)-nitrostyrene (**1a–1f**) is provided in Fig. 1.[29]

Among the various stereochemically relevant possibilities, the attack of the (*E*)-*anti*-enamine (using its *si*-face) on the *si*-face of nitrostyrene (**TS-1f**) is identified as energetically the most preferred transition state for the Michael addition. In fact, **TS-1f** is found to be relatively more stable by 5.0 kcal mol^{-1} than the nearest lower energy transition state (**TS-1a**), which leads to the (2*R*,3*R*) diastereomer. It can be noticed from the computed activation barriers (Table 1) that the bulky substituent at the α-position plays a steering role in promoting the Michael addition from the *anti*-enamine. The activation barriers associated with the *syn*-enamine additions are evidently higher than the corresponding *anti*-enamines. Further, the presence of a bulky α-substituent effectively shields the *re*-face of the (*E*)-*anti*-enamine from Michael acceptors. The most interesting consequence of the above features offered by the catalyst and the accompanying energetics is high precision diastereoselectivity. The lowest energy transition state **TS-1f** leads to (2*R*,3*S*) nitroalkane, which is in perfect accordance with the experimental reports.[30] The predicted enantiomeric excess

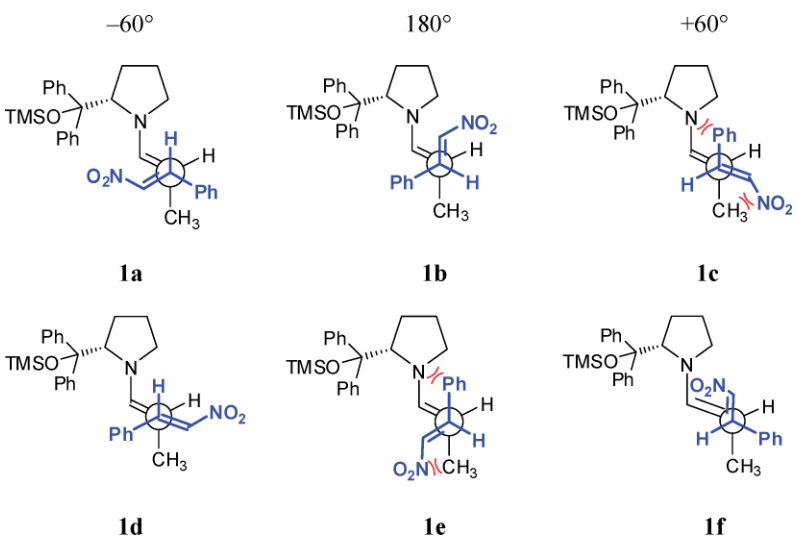

Fig. 1 Key conformers of the transition states for the first Michael addition of (*E*)-*anti*-enamine to the *re*/*si* face of nitrostyrene. These conformers are grouped on the basis of the dihedral angle between the enamine double bond and the hydrogen of the nitrostyrene (as indicated) with dihedral angles of –60°, +180° and +60°.

Table 1 The computed activation barriers ($\Delta E^{\ddagger}$) at the B3LYP/6-31G*//ONIOM2(B3LYP/6-31G*:AM1) level for the addition of enamines to (*E*)-nitrostyrene

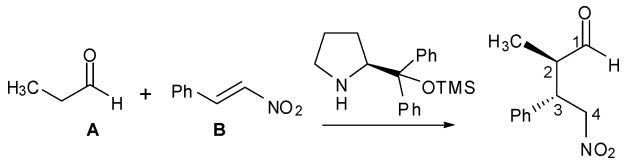

Enamine	Enamine-nitrostyrene prochiral faces	Product configuration	Transition state	$\Delta E^{\ddagger}$ in kcal mol^{-1}[a] Absolute	Relative
(*E*)-*anti*	*si*→*re*	*(R,R)*	**TS-1a**	28.4	5.0
	si→*re*	*(R,R)*	**TS-1b**	31.8	8.4
	si→*si*	*(R,S)*	**TS-1d**	31.7	8.3
	si→*si*	*(R,S)*	**TS-1f**	23.4	**0.0**
(*Z*)-*anti*	*re*→*re*	*(S,R)*	**TS-2a**	28.2	7.0
	re→*si*	*(S,S)*	**TS-2f**	29.1	7.9
(*E*)-*syn*	*re*→*re*	*(S,R)*	**TS-3a**	29.6	6.5
	re→*re*	*(S,R)*	**TS-3c**	33.3	10.2
	re→*si*	*(S,S)*	**TS-3e**	33.2	10.1
	re→*si*	*(S,S)*	**TS-3f**	33.6	10.5

[a] Absolute energy barriers are calculated with respect to the separated reactants and the relative energy barriers with respect to the energy of the lowest energy TS.

of >99% is found to be the same as the experimental reports by Hayashi *et al.* on the Michael addition between propanal enamine and nitrostyrene.[30]

While attempting to locate other transition state conformers for (*E*)-*anti*-enamine addition to the nitrostyrene, two important gauche interactions appeared quite prominent. These include the unfavorable interaction between (i) the phenyl ring on the electrophile and the pyrrolidine ring, (ii) the nitro on the electrophile and the methyl of the enamine moiety. In general, it is noticed that such interactions tend to increase the energy of the addition transition states. Further, repeated attempts to identify **1c** and **1e** (Fig. 2) resulted in rotation around the incipient C–C bond during geometry optimization and it was found that they reverted to the nearest lower energy transition states such as **TS-1a**

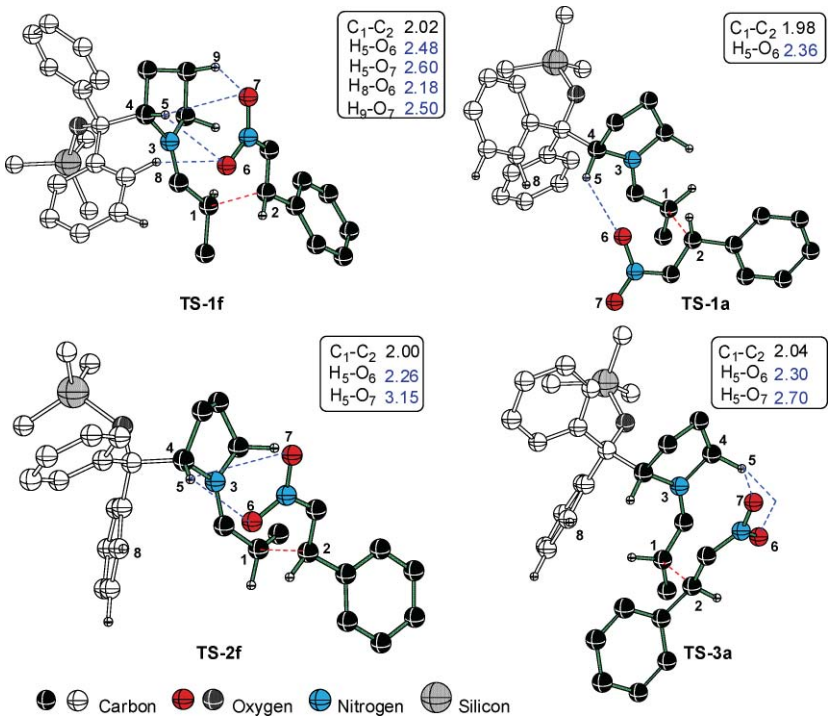

Fig. 2 The ONIOM2(B3LYP/6-31G*:AM1) optimized lower energy diastereomeric transition state geometries for the addition of enamine derived from the catalyst and propanal to (*E*)-nitrostyrene. Only selected hydrogens are shown for clarity. Distances are given in Å.

and **TS-1f**.[31] Interestingly, **TS-1a** and **TS-1f** are devoid of gauche interactions of the above kind. It is therefore evident that the substituents and geometries of the enamine and nitrostyrene exert a direct control on the stereochemical outcome of the reaction.

A number of stabilizing interactions are identified as responsible for the differential stabilization between the transition states. The developing nitroxide in **TS-1f** is found to be stabilized by a network of weak hydrogen bonding interactions as shown in Fig. 2. For instance, the distance between the methylene hydrogens of the pyrrolidine ring and the oxygens of the nitro group are between 2.5 and 2.6 Å. The optimized geometries of other diastereomeric transition states evidently reveal that the above-mentioned stabilizing interaction is not as effective as in **TS-1f**. Another noticeable stabilizing interaction in **TS-1f** is between the $-NO_2$ group and the aryl hydrogens of the α-substituent on the pyrrolidine ring. Such additional stabilizations in **TS-1f** are nearly absent in any other lower energy diastereomeric transition states. It is further noticed that the C-γ heads the envelope conformation of the pyrrolidine ring in **TS-1f**, whereas it is C-β in **TS-1a**. Hence in **TS-1f**, the C-γ hydrogen offers additional stabilization to the nitro group of the electrophile (as evident from the C–H $\cdots$ O distance of 2.5 Å). We have identified a bond path and the corresponding bond critical point (bcp) using the AIM theory for these interactions.[32] **TS-1a** on the other hand, lacks such additional weak interactions, except that due to the α-methylene of the pyrrolidine ring. Additionally, an electrostatic stabilization between the partially negative pyrrolidine nitrogen (developing iminium moiety in the TS) with the partially positive nitrogen of the electrophile is likely.[33] The $N^{\delta+} \cdots N^{\delta-}$ distance in **TS-1f** is found to be shorter (2.9 Å) than that in **TS-1a** (3.9 Å). In addition to the steric effects, hydrogen bonds, as described above, evidently contribute towards differentiating the diastereofacial approaches. All these factors contribute to the improved relative stabilization of **TS-1f**. On the basis of the analysis of intramolecular stabilizing interactions, as well as the computed activation barriers, it is now logical to state that the first step of this cascade reaction through **TS-1f** would lead to a high degree of stereocontrol.

More direct evidence in support of better kinetic preference of enamine towards nitrostyrene as opposed to enal (**C**) is gathered by separately evaluating the activation barriers for the addition. We have located transition states for the addition of enamine to α,β-unsaturated aldehyde. The calculated barriers are found to be higher by 7 kcal mol^{-1} than the lowest energy TS for the addition of enamine to nitrostyrene.[34] If the first Michael addition occurs between enamine and enal, the products are going to be significantly different as compared to what has been reported experimentally.[35] It can also be noticed that the Michael adduct formed between nitrostyrene and enamine is detected experimentally.[9,16b] The computed activation barriers reveal that the lowest energy pathway should involve the addition of enamine to nitrostyrene as the first step. Although the reaction between enamine and enal cannot be completely ruled out, the experimental observation along with the computed data, clearly justify the reaction sequence as beginning with the addition of enamine to nitrostyrene in this triple cascade reaction.

The generation of the third and fourth stereocentres takes place in the next step by the addition of the anion generated from the nitroalkane to the pre-activated enal (**C**).[36] The energetically more favored geometrical isomer of the iminium ion formed between enal (**C**) and the catalyst is found to have *E*,*s-trans*,*E* stereochemistry.[37] This stereoisomer is chosen for further calculations. The formation of iminium ion renders more electrophilic character to the β-carbon of the α,β-unsaturated enal, thereby facilitating the second Michael addition with the nitroalkane anion generated in the preceding step.[38] The α-substituent on the pyrrolidine now comes into play in effectively differentiating the enantiotopic faces of the iminium ion to the approaching nucleophile. Since the *re* face is effectively shielded, the nucleophilic attack takes place on the *si* face of the iminium ion. The transition states for the Michael addition of nitroalkane anion to (*E*,*s-trans*,*E*)-iminium are identified wherein the configuration of nitroalkane is retained as (2*R*,3*S*), which is the major stereoisomer from the preceding step (Fig. 2). It is to be reckoned that the last step involves an intramolecular aldol cyclization (Scheme 1). The geometric requirement that the enamine and the electrophile (the CHO group) should be in reasonable proximity leads to only a limited number of conformers for the corresponding transition states. The nitroalkane anion can add to the Michael acceptor (iminium ion) using either the *re* face or *si* face as shown in Fig. 3. Hence the second Michael addition will result in the formation of products with an epimeric carbon.

The calculated absolute and relative activation barriers, respectively, with respect to the pre-reacting complex (between the reactants) and the lowest energy TS are tabulated in Table 2. Among the various possible modes of addition, the transition state **TS-4b** involving *si*-facial attack by the nitroalkane anion on the *re* face of the iminium is found to be the most favored mode. The optimized geometry conveys that the nitro and phenyl groups respectively on nucleophile and electrophile tend to remain antiperiplanar in the lower energy transition states. In other conformations, such as in **4a** and **4c**, the relative positions between the nitro and the phenyl groups are found to be gauche. These conformers are evidently higher in energy than **TS-4b**.[39] Three key transition states are considered for the addition of the *re*-face of the nitroalkane anion to the *re*-face of the iminium ion. The optimized geometry of **TS-4e** is found to prefer a conformation where the iminium double bond eclipses the $-NO_2$ group.[40] Only two unique transition states could be identified. Interestingly, during the course of transition state geometry optimization, the initial guess geometry of **TS-4f** converges to a structure identical to that of **TS-4d**.[41] The optimized structures of the lowest energy transition states leading to the formation of epimeric products are provided in Fig. 4.

Analysis of the geometries of lower energy transition states revealed several interesting facts. In both diastereomeric transition states (**TS-4b**, **TS-4d**), a preference for a staggered arrangement of the substituents around the incipient C–C bond is evident from the C_{10}–C_1–C_2–H_{11} dihedral angle. The hydrogen bonding between the α-hydrogens on the pyrrolidine ring (H_5) and the $-NO_2$ group is found to be nearly the same in these transition states (Fig. 4). But a noticeable stabilizing interaction between the carbonyl oxygen and one of the methylene hydrogens of the pyrrolidine ring (O_9-H_8) is observed in **TS-4b**. The C=O $\cdots$ H distance is found to be 2.49 Å, implying a reasonably good hydrogen bonding stabilization. This interaction is totally absent in **TS-4d**, as the orientation of the carbonyl group is away from the pyrrolidine ring. Another interesting hydrogen bonding interaction is identified between the nitro group and the aryl

Table 2 The computed activation barriers ($\Delta E^{\ddagger}$) at the B3LYP/6-31G*//ONIOM2(B3LYP/6-31G*:AM1) level for the addition of a nitroalkane anion to the iminium derived from the enal (**C**)

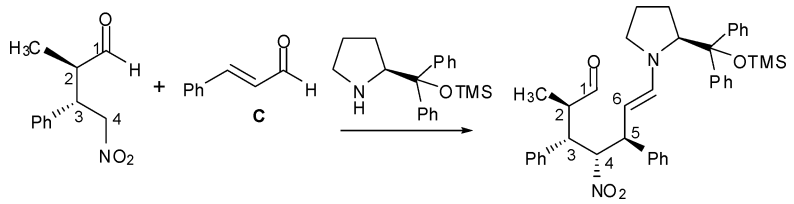

Transition state	Prochiral face of nitroalkane anion	$\Delta E^{\ddagger}$ in kcal mol^{-1}	
		Absolute [a]	Relative
TS-4b	*si*	5.4	0.0
TS-4c	*si*	7.8	4.2
TS-4f → TS-4d	*re*	11.7	2.2
TS-4e	*re*	2.8	2.5

[a] Here the absolute barrier refers to the energy difference between the respective pre-reacting complexes and corresponding transition states.

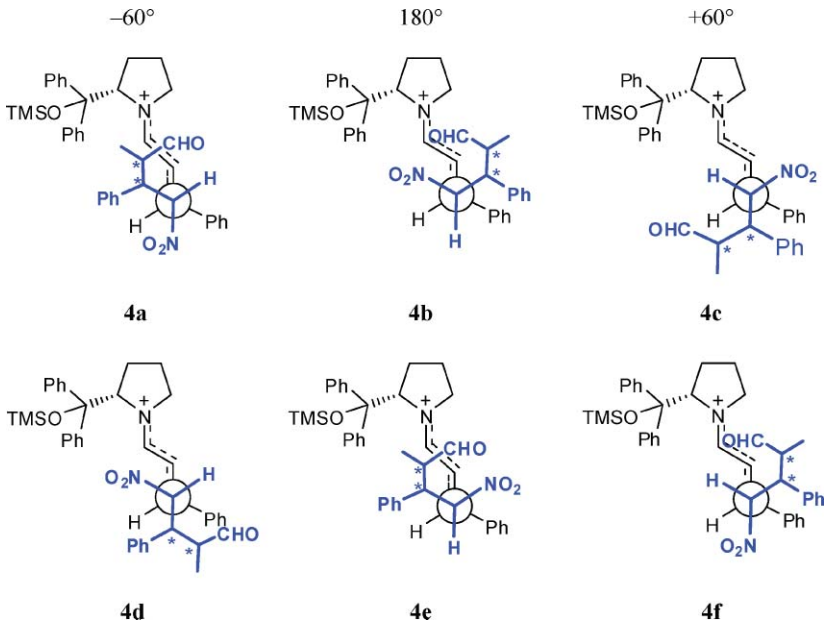

Fig. 3 Key conformers of the transition states for the second Michael addition step. These conformers are grouped on the basis of the dihedral angle between the iminium double bond and the hydrogen of the nitroalkane (as indicated) with dihedral angles of –60°, +180° and +60°.

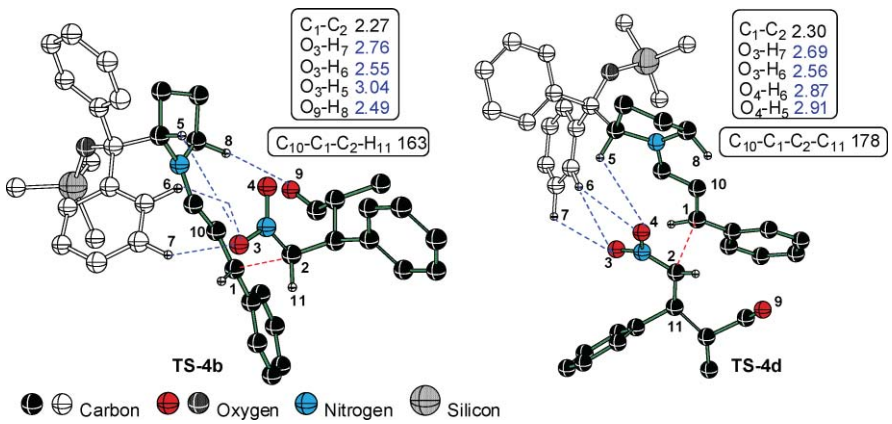

Fig. 4 The ONIOM2(B3LYP/6-31G*:AM1) optimized geometries of lower energy transition states for the second Michael addition step between the nitroalkane anion and the iminium ion (formed between pyrrolidine and α,β-unsaturated aldehyde). Only selected hydrogens are shown for clarity. Angles are given in degrees and distances in Å.

hydrogens of the pyrrolidine α-substituent as shown in Fig. 4.[32] This highlights the importance of weak stabilizing interactions offered by the α-substituent in contributing toward the extra stabilization of **TS-4b** and **TS-4d**, a feature that is lacking in all other transition state possibilities (**TS-4c**, **TS-4e**). Interestingly, the lower energy transition states in both Michael addition steps (**TS-1f**, **1a** and **TS-4b**, **4d**) in this cascade reaction exhibited the above stabilizing interaction. The cumulative effect of such interactions results in an energy difference of 2.2 kcal mol^{-1} between **TS-4b** and the diastereomeric **TS-4d**, which corresponds to a diastereomeric excess of 95% in favor of the (2*R*,3*S*,4*S*,5*S*)-2-methyl-4-nitro-3,5-diphenyl enamine intermediate. This prediction is in accordance with the experimental results obtained for diphenyl prolinol silyl ether catalyzed reactions between α,β-unsaturated aldehyde and γ-nitroketone.[15] However, quantitative agreement with the experimental observation (diastereomeric excess) could vary depending on the choice of theory and basis sets.[42]

The enamine thus formed should participate in an intramolecular aldol cyclization. A schematic representation indicating the key conformational possibilities is given in Fig. 5. The geometric requirement that the enamine and the electrophile stay in reasonable proximity for the aldol reaction to take place severely restricts the number of reactive conformers for the ensuing C–C bond-forming step. The enamine intermediate generated in the preceding Michael addition step through pathways **4a**, **4b**, and **4c** (Fig. 3) can in principle undergo ring closure either through **5a** or **5d**. Further, **5b** and **5c** correspond to possible transition states for the intramolecular aldol cyclization of the enamine precursors generated from **4d** and **4f**.

The optimized geometries of lower energy transition states for the intramolecular cyclization of the enamine intermediate are provided in Fig. 6. The lowest energy transition state (**TS-5a**)[43] is found to be 9.1 kcal mol^{-1} more stable than the other possibilities, such as **TS-5c**. Both these TSs are found to maintain a chair conformation where the nitro group and the phenyl ring occupy the axial positions. An additional methyl group at the axial position contributes to the higher energy of **TS-5c**.[44] Among the weak interactions stabilizing the developing alkoxide, the hydrogen

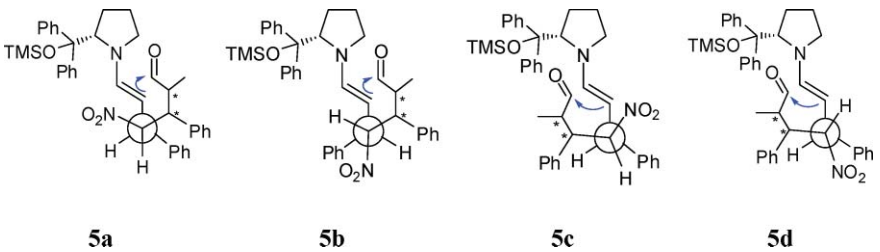

Fig. 5 Key conformers of the transition states for the intramolecular cyclization of the enamine with favorable geometric disposition between the aldehyde and enamine.

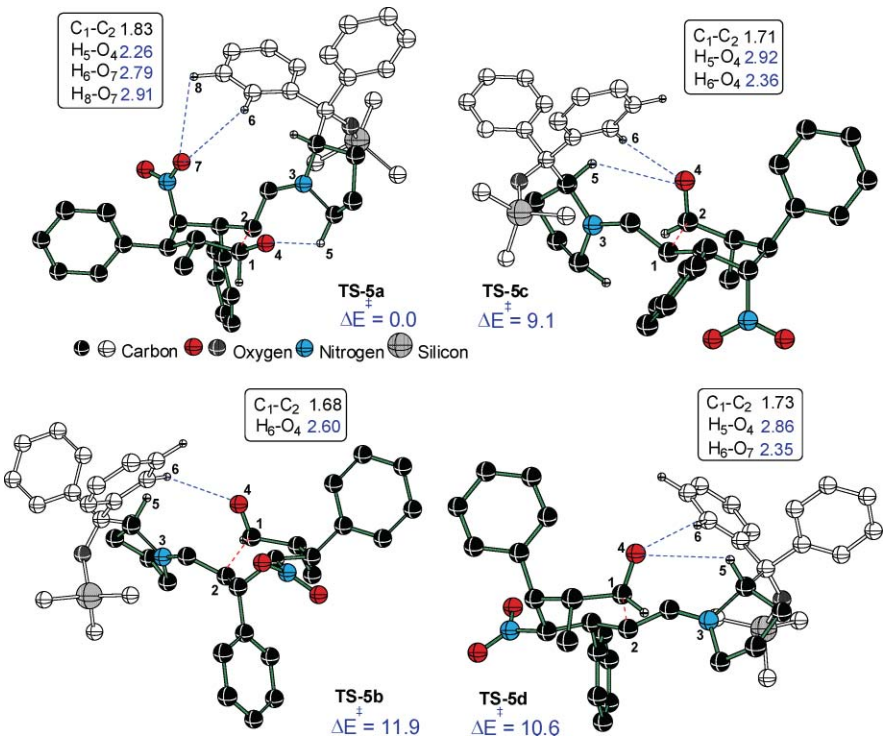

Fig. 6 The ONIOM2(B3LYP/6-31G*:AM1) optimized geometries for the lower energy transition states of intramolecular aldol cyclization. Only selected hydrogens are shown for clarity. Distances are given in Å. Relative energies ($\Delta E^{\ddagger}$ in kcal) are obtained at the B3LYP/6-31G*// ONIOM2(B3LYP/6-31G*:AM1) level of theory.

bonding between the Cα methylene hydrogen (adjacent to the pyrrolidine N) is more prominent in **TS-5a** with a distance of 2.26 Å than that in **TS-5c**, which has a distance of interaction of 2.92 Å.[32] An additional weak C–H(aryl) · · · O interaction in **TS-5a** arises due to the orientation of the nitro group towards the phenyl ring of the pyrrolidine substituent. On the basis of the computed energies, it is clear that the intramolecular aldol reaction through **TS-5a** would lead to ring closure. The cascade reaction eventually generates (3*S*,4*S*,5*R*,6*R*)-3-methyl-5-nitro-4,6-diphenyl cyclohex-1-ene carbaldehyde with four contiguous stereocentres with a high degree of stereoselectivity. This feature is evidently achieved by using a diphenyl prolinol silyl ether catalyst for promoting asymmetric Michael reactions in the cascade sequence.

Conclusions

Mechanistic features of an interesting triple cascade Michael–Michael–Aldol reaction towards the generation of a cyclohexene carbaldehyde have been established using density functional theory calculations. We have been able to shed light on the controlling factors responsible for the high stereoselectivity observed experimentally. This has been achieved by precisely identifying all the stereochemically relevant transition states for three most important C–C bond-forming reactions in the cascade reaction sequence. The reaction pathways for the first two asymmetric Michael additions proceed through enamine as well as iminium activation modes, respectively, for aldehyde and α,β-unsaturated enal. The examination of various stereochemically important modes of additions between enamine and nitrostyrene conveyed that the *si*-face of enamine (derived from the catalyst and propanal) adding to the *si*-face of nitrostyrene possesses the lowest activation energy. In the case of the second Michael addition step, the addition of the *si*-face of the nitroalkane anion to the *re*-face of the iminium ion (derived from enal and the catalyst) was found to be the lowest energy transition state. The predicted stereoselectivities are found to be in perfect concurrence with the experimental observation as reported by Enders and co-workers. The present results support the steric control approach, wherein efficient shielding of one face of the iminium/enamine intermediates is crucial to high levels of asymmetric induction. We anticipate that these insights into how stereoselectivity is achieved in a triple cascade reaction could be useful in designing novel one pot sequences towards highly complex target molecules.

Acknowledgements

We thank the Department of Science and Technology (DST), New Delhi for financial support (through SR/S1/OC-50/2003) and the IITB computer centre for generous computing facilities. SCB acknowledges CSIR New Delhi for the senior research fellowship.

References

1 (*a*) D. J. Ramón and M. Yus, *Angew. Chem., Int. Ed.*, 2005, **44**, 1602; (*b*) H.-C. Guo and J.-A. Ma, *Angew. Chem., Int. Ed.*, 2006, **45**, 354.
2 (*a*) P. J. Parson, C. S. Penkett and A. J. Shell, *Chem. Rev.*, 1996, **96**, 195; (*b*) L. F. Tietze, *Chem. Rev.*, 1996, **96**, 115; (*c*) K. C. Nicolaou, T. Montagnon and S. A. Snyder, *Chem. Commun.*, 2003, 551; (*d*) H. Pellisier, *Tetrahedron*, 2006, **62**, 2143; (*e*) D. Enders, C. Grondal and M. R. M. Hüttl, *Angew. Chem., Int. Ed.*, 2007, **46**, 1570.
3 (*a*) P. I. Dalko and L. Moisan, *Angew. Chem., Int. Ed.*, 2001, **40**, 3726; (*b*) P. I. Dalko and L. Moisan, *Angew. Chem., Int. Ed.*, 2004, **43**, 5138; (*c*) D. B. Ramachary and C. F. Barbas III, *Chem.–Eur. J.*, 2004, **10**, 5323; (*d*) J. Seayad and B. List, *Org. Biomol. Chem.*, 2005, **3**, 719; (*e*) M. J. Gaunt, C. C. C. Johansson, A. McNally and N. T. Vo, *Drug Discovery Today*, 2007, **12**, 8.
4 (*a*) Y. Huang, A. M. Walji, C. H. Larsen and D. W. C. MacMillan, *J. Am. Chem. Soc.*, 2005, **127**, 15051; (*b*) Y. Hayashi, T. Okano, S. Aratake and D. Hazelard, *Angew. Chem., Int. Ed.*, 2007, **46**, 4922; (*c*) L. Zu, H. Xie, J. Wang, W. Jiang, Y. Tang and W. Wang, *Angew. Chem., Int. Ed.*, 2007, **46**, 3732.
5 (*a*) K. C. Nicolaou, D. J. Edmonds and P. G. Bulger, *Angew. Chem., Int. Ed.*, 2006, **45**, 7134; (*b*) S.-L. Cui, X.-F. Lin and Y.-C. Wang, *Eur. J. Org. Chem.*, 2006, 5174.
6 (*a*) A. B. Northrup and D. W. C. MacMillan, *J. Am. Chem. Soc.*, 2002, **124**, 2458; (*b*) I. K. Mangion, A. B. Northrup and D. W. C. Macmillan, *Angew. Chem., Int. Ed.*, 2004, **43**, 6722; (*c*) B. List, *Acc. Chem. Res.*, 2004, **37**, 548; (*d*) B. List, *Chem. Commun.*, 2006, 819; (*e*) A. Erkkilä, I. Majander and P. M. Pihko, *Chem. Rev.*, 2007, **107**, 5416; (*f*) S. Mukherjee, J. W. Yang, S. Hoffmann and B. List, *Chem. Rev.*, 2007, **107**, 5471.
7 (*a*) B. List, P. Pojarliev and H. J. Martin, *Org. Lett.*, 2001, **3**, 2423; (*b*) C. Allemann, R. Gordillo, F. R. Clemente, P. H.-Y. Cheong and K. N. Houk, *Acc. Chem. Res.*, 2004, **37**, 558.
8 C. Palomo and A. Mielgo, *Angew. Chem., Int. Ed.*, 2006, **45**, 7876.
9 D. Enders, M. R. M. Huttl, C. Grondal and G. Raabe, *Nature*, 2006, **441**, 861.
10 (*a*) M. Marigo, J. Franzén, T. B. Poulsen, W. Zhuang and K. A. Jørgensen, *J. Am. Chem. Soc.*, 2005, **127**, 6964; (*b*) J. Franzén, M. Marigo, D. Fielenbach, T. C. Wabnitz, A. Kjærsgaard and K. A. Jørgensen, *J. Am. Chem. Soc.*, 2005, **127**, 18296; (*c*) Y. Chi and S. H. Gellman, *Org. Lett.*, 2005, **7**, 4253; (*d*) G.-L. Zhao and A. Córdova, *Tetrahedron Lett.*, 2006, **47**, 7417; (*e*) A. Carlone, M. Marigo, C. North, A. Landa and K. A. Jørgensen, *Chem. Commun.*, 2006, 4928; (*f*) C. Palomo, S. Vera, I. Velilla, A. Mielgo and E. Gómez-Bengoa, *Angew. Chem., Int. Ed.*, 2007, **46**, 8054.
11 (*a*) M. Marigo, T. Schulte, J. Franzén and K. A. Jørgensen, *J. Am. Chem. Soc.*, 2005, **127**, 15710; (*b*) M. Marigo, S. Bertelsen, A. Landa and K. A. Jørgensen, *J. Am. Chem. Soc.*, 2006, **128**, 5475; (*c*) W. Wang, H. Li, J. Wang and L. Zu, *J. Am. Chem. Soc.*, 2006, **128**, 10354; (*d*) S. Brandau, E. Maerten and K. A. Jørgensen, *J. Am. Chem. Soc.*, 2006, **128**, 14986; (*e*) D. B. Ramachary and M. Kishor, *J. Org. Chem.*, 2007, **72**, 5056; (*f*) A. Carlone, S. Cabrera, M. Marigo and K. A. Jørgensen, *Angew. Chem., Int. Ed.*, 2007, **46**, 1101.
12 (*a*) For such Michael additions, nitrostyrenes in general are found to be very effective: D. Enders and A. Seki, *Synlett*, 2002, 26; (*b*) O. M. Berner, L. Tedeshi and D. Enders, *Eur. J. Org. Chem.*, 2002, 1877; (*c*) R. Ballini, G. Bosica, D. Fiorini, A. Palmieri and M. Petrini, *Chem. Rev.*, 2005, **105**, 933; (*d*) D. Enders and S. Chow, *Eur. J. Org. Chem.*, 2006, 4578; (*e*) S. B. Tsogoeva, *Eur. J. Org. Chem.*, 2007, 1701; (*f*) K. Albertshofer, R. Thayumanavan, N. Utsumi, F. Tanaka and C. F. Barbas III, *Tetrahedron Lett.*, 2007, **48**, 693.
13 (*a*) O. Andrey, A. Alexakis, A. Tomassini and G. Bernardinelli, *Adv. Synth. Catal.*, 2004, **346**, 1147; (*b*) T. Ishii, S. Fujioka, Y. Sekiguchi and H. Kotsuki, *J. Am. Chem. Soc.*, 2004, **126**, 9558; (*c*) W. Wang, J. Wang and H. Li, *Angew. Chem., Int. Ed.*, 2005, **44**, 1369.
14 (*a*) Significant recent developments in organocatalytic Michael reactions involving enamine or iminium intermediates have been reported; (*b*) D. Almaşi, D. A. Alonso and C. Nájera, *Tetrahedron: Asymmetry*, 2007, **18**, 299; (*c*) J. L. Vicario, D. Badía and L. Carrillo, *Synthesis*, 2007, **14**, 2065; (*d*) S. Hanessian and V. Pham, *Org. Lett.*, 2000, **2**, 2975; (*e*) N. Halland, R. G. Hazell and K. A. Jørgensen, *J. Org. Chem.*, 2002, **67**, 8331; (*f*) N. Halland, P. S. Aburel and K. A. Jørgensen, *Angew. Chem., Int. Ed.*, 2003, **42**, 661; (*g*) A. Prieto, N. Halland and K. A. Jørgensen, *Org. Lett.*, 2005, **7**, 3897; (*h*) H. Gotoh, H. Ishikawa and Y. Hayashi, *Org. Lett.*, 2007, **9**, 5307.
15 D. Enders, A. A. Narine, T. R. Benninghaus and G. Raabe, *Synlett*, 2007, **11**, 1667.
16 (*a*) D. Enders, M. R. M. Hüttl, J. Runsink, G. Raabe and B. Wendt, *Angew. Chem., Int. Ed.*, 2007, **46**, 467; (*b*) D. Enders, M. R. M. Hüttl, G. Raabe and J. W. Bats, *Adv. Synth. Catal.*, 2008, **350**, 267.
17 (*a*) D. Roy and R. B. Sunoj, *Org. Lett.*, 2007, **9**, 4873; (*b*) M. P. Patil and R. B. Sunoj, *J. Org. Chem.*, 2007, **72**, 8202; (*c*) D. Janardanan and R. B. Sunoj, *J. Org. Chem.*, 2007, **72**, 331; (*d*) D. Janardanan and R. B. Sunoj,

Chem.–Eur. J., 2007, **13**, 4805; (*e*) C. B. Shinisha and R. B. Sunoj, *Org. Biomol. Chem.*, 2007, **5**, 1287.
18 (*a*) S. Dapprich, I. Komáromi, K. S. Byun, K. Morokuma and M. J. Frisch, *J. Mol. Struct. (THEOCHEM)*, 1999, **461–462**, 1; (*b*) T. Vreven and K. Morokuma, *J. Comput. Chem.*, 2000, **21**, 1419; (*c*) K. Morokuma, *Bull. Korean Chem. Soc.*, 2003, **24**, 797; (*d*) K. Morokuma, *Philos. Trans. R. Soc. London, Ser. A*, 2002, **360**, 1149; (*e*) T. Vreven, K. S. Byun, I. Komáromi, S. Dapprich, J. A. Montgomery, Jr., K. Morokuma and M. J. Frisch, *J. Chem. Theory Comput.*, 2006, **2**, 815.
19 M. J. Frisch, G. W. Trucks, H. B. Schlegel, G. E. Scuseria, M. A. Robb, J. R. Cheeseman, J. A. Montgomery, Jr., T. Vreven, K. N. Kudin, J. C. Burant, J. M. Millam, S. S. Iyengar, J. Tomasi, V. Barone, B. Mennucci, M. Cossi, G. Scalmani, N. Rega, G. A. Petersson, H. Nakatsuji, M. Hada, M. Ehara, K. Toyota, R. Fukuda, J. Hasegawa, M. Ishida, T. Nakajima, Y. Honda, O. Kitao, H. Nakai, M. Klene, X. Li, J. E. Knox, H. P. Hratchian, J. B. Cross, V. Bakken, C. Adamo, J. Jaramillo, R. Gomperts, R. E. Stratmann, O. Yazyev, A. J. Austin, R. Cammi, C. Pomelli, J. Ochterski, P. Y. Ayala, K. Morokuma, G. A. Voth, P. Salvador, J. J. Dannenberg, V. G. Zakrzewski, S. Dapprich, A. D. Daniels, M. C. Strain, O. Farkas, D. K. Malick, A. D. Rabuck, K. Raghavachari, J. B. Foresman, J. V. Ortiz, Q. Cui, A. G. Baboul, S. Clifford, J. Cioslowski, B. B. Stefanov, G. Liu, A. Liashenko, P. Piskorz, I. Komaromi, R. L. Martin, D. J. Fox, T. Keith, M. A. Al-Laham, C. Y. Peng, A. Nanayakkara, M. Challacombe, P. M. W. Gill, B. G. Johnson, W. Chen, M. W. Wong, C. Gonzalez and J. A. Pople, *GAUSSIAN 03 (Revision C.02)*, Gaussian, Inc., Wallingford, CT, 2004.
20 (*a*) T. Dudding and K. N. Houk, *Proc. Natl. Acad. Sci. U. S. A.*, 2004, **101**, 5770; (*b*) V. P. Ananikov, R. Szilagyi, K. Morokuma and D. G. Musaev, *Organometallics*, 2005, **24**, 1938; (*c*) D. Balcells, F. Maseras and G. Ujaque, *J. Am. Chem. Soc.*, 2005, **127**, 3624; (*d*) X. Zhang, H. Du, Z. Wang, Y.-D. Wu and K. Ding, *J. Org. Chem.*, 2006, **71**, 2862.
21 (*a*) A. D. Becke, *J. Chem. Phys.*, 1993, **98**, 5648; (*b*) A. D. Becke, *Phys. Rev. A*, 1998, **38**, 3098; (*c*) C. Lee, W. Yang and R. G. Parr, *Phys. Rev. B*, 1998, **37**, 785.
22 (*a*) R. Ditchfield, W. J. Hehre and J. A. Pople, *J. Chem. Phys.*, 1971, **54**, 724; (*b*) W. J. Hehre, R. Ditchfield and J. A. Pople, *J. Chem. Phys.*, 1972, **56**, 2257; (*c*) P. C. Hariharan and J. A. Pople, *Theor. Chim. Acta*, 1973, **28**, 213.
23 Two-layered ONIOM partition scheme for the catalyst is given in Fig. S1 (ESI†).
24 The geometric parameters are summarized in Table S1 in the ESI.† The average correlation coefficient (R^2) for the important structural parameters obtained through full B3LYP and ONIOM2 (B3LYP:AM1) optimized geometries for the catalyst is found to be 0.9.
25 Different conformations arising due to the rotation of the α-substituent around the pyrrolidine ring are considered. The most favored conformer is found to have a dihedral angle of +60° between the N–C(2) and C–O bond of the substituent. This geometry is found to be relatively more stable by 2.9 kcal mol^{-1} than the next highest energy conformer. See Table S2 in the ESI for the relative energies of various conformers of the catalyst. The ring conformational features of the catalyst are not investigated in this study.
26 (*a*) The computed GRDs are found to be evidently in favor of nitrostyrene as the preferred electrophile to react with the enamine rather than enal. The computed electronegativity (χ), hardness (η) and electrophilicity index (ω) are tabulated in Table S5 (ESI). R. G. Parr and R. G. Pearson, *J. Am. Chem. Soc.*, 1983, **105**, 7512; (*b*) W. Yang and W. J. Mortier, *J. Am. Chem. Soc.*, 1986, **108**, 5708; (*c*) R. G. Parr, L. v. Szentpály and S. Liu, *J. Am. Chem. Soc.*, 1999, **121**, 1922; (*d*) H. Chermette, *J. Comput. Chem.*, 1999, **20**, 129; (*e*) L. R. Domingo, P. Pérez and R. Contreras, *Tetrahedron*, 2004, **60**, 6585.
27 (*a*) The (*E*)-isomer of the electrophile is found to be energetically more stable. This orientation is maintained in the present study; (*b*) For experimental evidence see T. Ohwada, T. Ohta and K. Shudo, *J. Am. Chem. Soc.*, 1986, **108**, 3029.
28 See Table S3 for the relative energies of *E*/*Z* isomers of *syn*/*anti*-enamines formed between the catalyst and propanal.
29 Other possible conformers for the addition of (i) (*Z*)-*anti*-enamine to (*E*)-nitrostyrene (**2a–2f**) and (ii) (*E*)-*syn*-enamine to (*E*)-nitrostyrene (**3a–3f**) are given in Fig. S2 in the ESI.
30 Y. Hayashi, H. Gotoh, T. Hayashi and M. Shoji, *Angew. Chem., Int. Ed.*, 2005, **44**, 4212.
31 Some of the possible conformers for the addition transition states of (*Z*)-*anti*-enamine and (*E*)-nitrostyrene as well as (*E*)-*syn*-enamine and (*E*)-nitrostyrene (**2b–e** and **3b**,**d** as in Fig. S2 in the ESI) could not be located. For more details, see the ESI.
32 (*a*) The electron density at the *bcp* along the key stabilizing interactions is provided in Fig. S3 of the ESI; (*b*) R. F. W. Bader, *Atoms in Molecules: A Quantum Theory*, Clarendon Press, Oxford, 1990; (*c*) *AIM2000*, version 2.0; The Buro fur Innovative Software, SBK-Software, Bielefeld, Germany.
33 Partial charges on nitrogens rendering electrostatic interaction are confirmed by examining the corresponding Mulliken as well as natural charges. Details of MCA and NPA analyses are provided in Table S4 (ESI†).
34 We located TSs for the addition of enamine to iminium formed by the α,β-unsaturated aldehyde. Although the activation barrier is less compared to other pathways, the product formed is highly unstable. Hence this pathway involving such double activation is likely to be very reversible. Moreover, entropic disadvantages are going to be higher as well. See Table S6 (ESI) for the optimized geometries and energetics of lower energy TSs for the addition of enamine to enal.
35 Plausible pathways leading to such products are provided in the ESI (Fig. S4).
36 In this step of the cascade reaction sequence, the third reactant, namely α,β-unsaturated aldehyde, first forms an iminium ion with the catalyst. This serves as the Michael acceptor for the C–C bond formation.
37 (*a*) Important geometrical isomers of the iminium ion are individually optimized. The (*E,s-trans,E*) isomer is found to be more stable than the (*Z,s-trans,E*) geometrical isomer by 1.5 kcal mol^{-1}; (*b*) Relative energies of possible isomers of the iminium ion are given in Table S6 in the ESI.
38 (*a*) P. Melchiorre and K. A. Jørgensen, *J. Org. Chem.*, 2003, **68**, 4151; (*b*) S. Bertelsen, M. Marigo, S. Brandes, P. Dinér and K. A. Jørgensen, *J. Am. Chem. Soc.*, 2006, **128**, 12973.
39 Even after repeated attempts, we could not locate the TS corresponding to conformer **4a**. The destabilizing interaction between the phenyl group of the pyrrolidine α-substituent and the substituents on nitroalkane is found to be prominent. It is therefore safe enough to assume that **4a** would be a higher energy conformer. All our initial guess geometries have developed oscillatory behavior, leading to lack of convergence or resulting in rotation around the incipient C–C bond towards **4c** during geometry optimization. This situation would not affect the conclusions drawn on the stereoselectivities.
40 In spite of repeated attempts, all initial guess transition state geometries with a staggered orientation of substituents around the incipient C–C bond (**4e** in Fig. 4) converge to an eclipsed conformation during geometry optimization.
41 Several attempts toward optimizing **TS-4f** have been carried out. These include constrained optimization of the key dihedral angles, a range of initial guess geometries with a number of local rotamers *etc.*. Invariably, all such efforts eventually cascaded down to **TS-4d**.
42 By using single-point energies at the B3LYP/6-31+G*//ONIOM2-(B3LYP/6-31G*:AM1) and B3LYP/6-31+G**//ONIOM2(B3LYP/6-31G*:AM1) levels, the computed relative energies of all the TSs for the first and second step of the reaction are found to show some variations with respect to the numbers obtained using the 6-31G* basis set. For comparison between these results, see Table S9 and S10 of the ESI.
43 We could not locate **TS-5a** using the ONIOM2 method. Optimizations were therefore carried out at the HF/6-31G* level. Relative energies and activation barriers were then computed by evaluating single-point energy at the B3LYP/6-31G* level.
44 Absolute and relative activation barriers for the intramolecular aldol cyclization are tabulated in Table S8 (ESI†).